


Shallow and Deep States of Beryllium Acceptor in GaN: Why Photoluminescence Experiments Do Not Reveal Small Polarons for Defects in Semiconductors

D. O. Demchenko¹, M. Vorobiov¹, O. Andrieiev¹, T. H. Myers², and M. A. Reshchikov¹

¹*Department of Physics, Virginia Commonwealth University, Richmond, Virginia 23220, USA*

²*Materials Science, Engineering, and Commercialization Program, Texas State University, San Marcos, Texas 78666, USA*

 (Received 26 May 2020; revised 28 August 2020; accepted 10 December 2020; published 13 January 2021)

Currently, only one shallow acceptor (Mg) has been discovered in GaN. Here, using photoluminescence (PL) measurements combined with hybrid density functional theory, we demonstrate that a shallow effective-mass state also exists for the Be_{Ga} acceptor. A PL band with a maximum at 3.38 eV reveals a shallow Be_{Ga} acceptor level at 113 ± 5 meV above the valence band, which is the lowest value among any dopants in GaN reported to date. Calculations suggest that the Be_{Ga} is a dual-nature acceptor with the “bright” shallow state responsible for the 3.38 eV PL band, and the “dark,” strongly localized small polaronic state with a significantly lower hole capture efficiency.

DOI: [10.1103/PhysRevLett.126.027401](https://doi.org/10.1103/PhysRevLett.126.027401)

Gallium nitride (GaN) is an essential material for modern light-emitting, high-power, and high-frequency devices [1]. Although *n*-type GaN can be easily produced by doping with Si or Ge, the production of high-quality conductive *p*-type GaN is still a challenging problem. Currently, the only *p*-type dopant in GaN is magnesium substituting for Ga atom (Mg_{Ga}). However, a relatively high ionization energy (0.22 eV) [2] of the Mg_{Ga} requires high doping concentrations to achieve *p*-type conductivity suitable for practical applications. Therefore, a shallow *p*-type dopant with the ionization energy lower than that of Mg_{Ga} is highly desirable.

Recent first-principles calculations predict the 0/– transition level of the Be_{Ga} at 0.45–0.65 eV above the valence band maximum [3–5]. The deep acceptor level originates from the small polaron nature of the Be_{Ga} defect state, i.e., localized hole self-trapped by significant lattice distortions. The optical transition via this state is predicted to have a maximum at 1.5–1.8 eV [3–6]. This behavior is typical for a wide range of defects in nitrides and oxides [3,7,8]. However, a controversy remains: on one hand, a successful *p*-type doping by Be has not been demonstrated and Be-doped GaN is usually semi-insulating. On the other hand, there is no experimental evidence for the deep acceptor state of Be_{Ga} predicted by theory.

Early photoluminescence (PL) studies of Be-doped GaN grown by molecular beam epitaxy revealed two Be-related luminescence bands: the ultraviolet (UVL_{Be}) and yellow (YL_{Be}) bands. The UVL_{Be} band consists of the zero-phonon line (ZPL) at 3.38 eV followed by a series of LO phonon replicas. The corresponding acceptor ionization energy was estimated between 60 and 250 meV [9–13], with a large uncertainty due to the unreliable identification of the type of transitions. The YL_{Be} band, which was recently attributed to the $\text{Be}_{\text{Ga}}\text{O}_{\text{N}}$ complex [14], has a

Gaussian-like shape with a maximum at about 2.2 eV and full width at half maximum (FWHM) of about 0.5 eV [15]. The predicted red PL band (with a maximum at 1.5–1.8 eV) has not been observed in PL experiments. In particular, the background signal at these photon energies was more than 2 orders of magnitude weaker than the UVL_{Be} band [11]. Electron paramagnetic resonance (EPR) studies on Be-doped GaN initially proposed the Be_{Ga} acceptor level at 0.7 eV above the valence band maximum (VBM) [16], which seemed to confirm the deep nature of the Be_{Ga} acceptor. However, later the authors revised their explanation and concluded that the photo-EPR signal originated from the carbon acceptor C_{N} [17], once again casting doubt about the deep versus shallow nature of the Be_{Ga} .

In this Letter, we demonstrate the existence of the shallow state of Be acceptor and explain the absence of the deep polaronic state in PL experiments. Experiment and calculations suggest that transitions via the polaronic state are suppressed by the low hole capture efficiency of the polaronic state. This resolves the seeming contradiction between theoretical predictions of the deep state and experimental observations of the shallow state of the Be_{Ga} acceptor.

The details of the samples, experimental, and theoretical methods are given in Ref. [18]. The high-energy portion of the PL spectrum of Be doped GaN is shown in Fig. 1. The near band edge (NBE) emission is dominated by a peak at 3.478 eV, which is attributed to the donor-bound exciton (DBE) recombination [2]. The peaks at about 3.46 eV are identified as the two-electron satellites (TES) that appear when the DBE annihilates, leaving the donor electron in one of the excited states [2]. The kink on the high energy side of the DBE line, at 3.484 eV, can be better resolved at 55 K and is attributed to the free exciton (FE). At lower photon energies, the PL spectrum is dominated by the

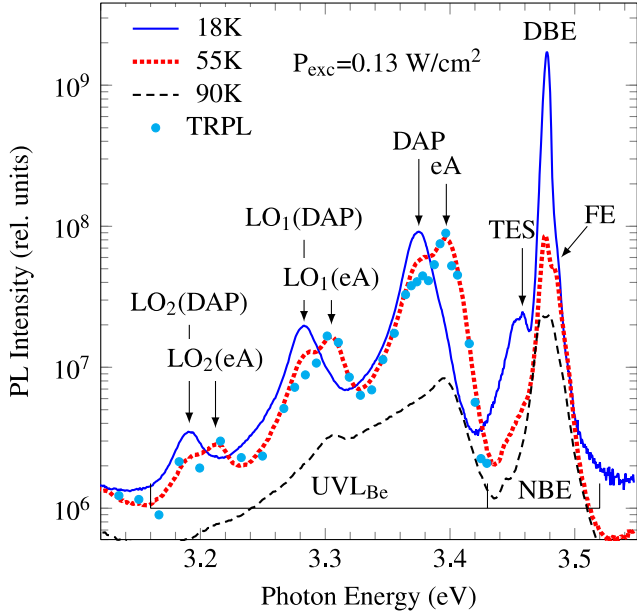


FIG. 1. Evolution of the PL spectrum with temperature for GaN:Be (sample 0408b) at $P_{\text{exc}} = 0.13 \text{ W/cm}^2$. The DAP peaks with the ZPL at 3.375 eV transform to identical in shape eA peaks with the ZPL at 3.395 eV. The LO phonon replicas follow the ZPL. The NBE emission consists of the two-electron satellite (TES), donor-bound exciton (DBE) and free exciton (FE) peaks. The time-resolved PL spectrum is shown with filled circles for the time-delay of 14 μs at $T = 55 \text{ K}$.

UVL_{Be} band, which we attribute to the Be_{Ga} acceptor. At $T = 18 \text{ K}$, the UVL_{Be} band is caused by electron transitions from shallow donors to the Be_{Ga} acceptor, the so-called donor-acceptor pair (DAP) transitions. The strongest peak at 3.375 eV is the ZPL (FWHM = 23 meV), which is followed by two LO phonon replicas separated by 92 meV. The Huang-Rhys factor estimated from the shape of the band is 0.2, a value typical for shallow acceptors, and lower than that for the Mg_{Ga} (0.4) [2]. With increasing excitation intensity P_{exc} from 10^{-5} to 0.1 W/cm^2 at $T = 18 \text{ K}$, the UVL_{Be} band shifts to higher energies by 6 meV, which agrees with its DAP nature.

It is expected that the DAP recombination mechanism is replaced with the eA mechanism (transitions from the conduction band to the same acceptor) with increasing temperature [2]. The temperature behavior of the UVL_{Be} band is shown in Fig. 1. With increasing temperature from 18 to 55 K, the DAP component of the UVL_{Be} band gradually disappears, and the eA component, with identical shape but shifted to higher energies by 20 meV, emerges. The ZPL of the eA-related band at 3.395 eV can be used to find the ionization energy of the Be_{Ga} acceptor, E_A precisely. By taking the difference between the FE and eA peaks and adding the FE binding energy (25 meV) [27], we obtained $E_A = 113 \pm 5 \text{ meV}$ from analysis of PL spectra at different temperatures in samples where these peaks are well resolved.

At $T = 55 \text{ K}$, time-resolved PL spectrum reveals the eA component of the UVL_{Be} band (Fig. 1). The decay of PL is slow, so that the signal can be traced up to hundreds of μs . While the DAP-associated shift of the UVL_{Be} peak was reported in the past, the replacement of the DAP component with the eA component with increasing temperature is observed for the first time. Such transformation is very similar to that observed for the Mg_{Ga}, Zn_{Ga}, and C_N acceptors in GaN, which are responsible for the UVL, BL1, and YL1 bands, respectively [2,19,28]. Considering the clear transformation of the DAP component to the eA component, the slow decay of PL after a laser pulse, the very low E_A , and the lowest Huang-Rhys factor among all known acceptors in GaN, all of these features indicate that Be_{Ga} is the shallowest acceptor in GaN known to date.

To understand the nature of the shallow Be_{Ga} acceptor in GaN, we construct the configuration coordinate diagram for this defect (Fig. 2), using the defect energies computed using Heyd-Scuseria-Ernzerhof (HSE) hybrid functional [20], and mapping the displacements ΔR_i of atom masses m_i onto a one-dimensional configuration coordinate Q as $\Delta Q^2 = \sum_{i,x,y,z} m_i \Delta R_i^2$ [21]. Absorption of a photon above the band gap creates an electron-hole pair, raising the energy of the system by $E_g = 3.5 \text{ eV}$ (dashed adiabatic potential labeled Be_{Ga}⁻ + E_g). Similarly to the case of the Mg_{Ga} acceptor [22], HSE calculations show that the neutral Be_{Ga} acceptor exhibits two very different defect states: a shallow effective-mass state at 0.24 eV above the VBM, and a deep polaronic state at 0.58 eV above the VBM. Note that Fig. 2 shows these defect states in two different

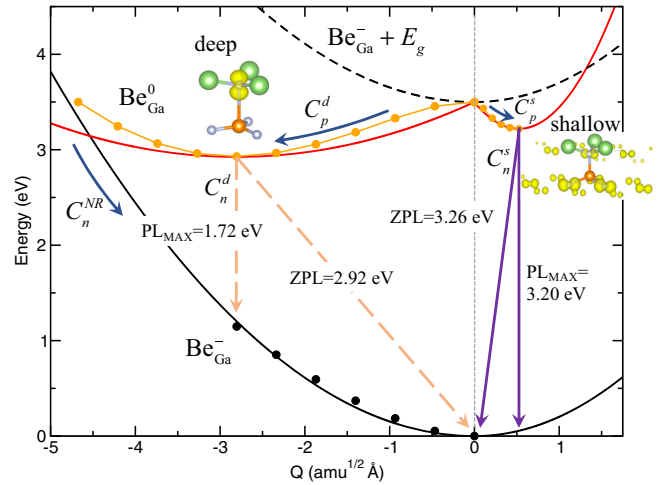


FIG. 2. Configuration coordinate diagram for the Be_{Ga} acceptor in GaN. The adiabatic potentials are obtained by fitting into HSE computed transition energies using the harmonic approximation. Direct HSE calculations are also performed (filled circles). Isosurfaces (at 10% of the maximum values) of the hole spin density for both shallow and deep states are shown (yellow) along with Be_{Ga} nearest neighbors. Small (gray) atoms are N, medium (orange) atoms are Be, and large (green) atoms are Ga.

directions of Q . Isosurfaces of the hole spin density show that in the deep polaronic state, the hole wave function is localized on the nearest nitrogen neighbor, with Be—N bond length increased by 0.7 Å from its equilibrium value. Small polaron states can be localized on any of the four nearest nitrogen atoms, with very similar lattice distortions and energies. The shallow state has the atomic configuration similar to that of the negative ground state, with a weakly localized hole. The calculated energy of the deep polaronic state of the Be_{Ga}^0 is 0.34 eV lower than that of the shallow state. A photogenerated hole can be captured by either of these two states, as shown by the arrows C_p^s and C_p^d in Fig. 2. The adiabatic potentials for the $\text{Be}_{\text{Ga}}^- + E_g$ and both Be_{Ga}^0 states intersect at $Q = 0$ (Fig. 2), where the neutral defect state eigenvalue is resonant with the valence band. Direct HSE calculations also show that there is no barrier for either state to capture the hole.

The above HSE calculations predict two PL bands (Fig. 2). First is a sharp line in the ultraviolet part of the spectrum with the PL maximum and ZPL at 3.20 and 3.26 eV, respectively (calculated Huang-Rhys factor is 2.8). Second is a very broad red PL band from the deep polaronic state with the PL maximum and ZPL at 1.72 and 2.92 eV, respectively (calculated Huang-Rhys factor is 32), in agreement with recent HSE calculations [3,4]. The experimental value of the ZPL for the UVL_{Be} band is 3.38 eV, in a reasonable agreement with the HSE calculations. However, as stated above, experiments do not reveal the predicted broad red band associated with the polaronic state.

The above apparent contradiction can be resolved by comparing the rates of electron and hole capture by the two defect states. Note that transitions via the shallow state must be radiative since there is no route for nonradiative transitions in this case, the potential curves of the neutral shallow and negative ground states do not intersect. Transitions via the deep state could be either radiative or nonradiative, depending on the width and height of the potential barrier formed by the intersection of the polaronic and the ground states potentials. To understand the optical properties of the Be_{Ga} acceptor, we calculate carrier capture coefficients (Fig. 2), which define the rates of transitions as $C_{n,p} = Vr$, where r is the capture rate of a carrier by one defect in a supercell with volume V .

Nonradiative transitions can be analyzed using the method proposed by Alkauskas *et al.* [21], where nonradiative transitions occur via multiphonon emission between the initial χ_i and the final χ_f vibronic states of two harmonic adiabatic potentials. The transition rate, in this case, can be computed as

$$r = f(T) \frac{2\pi}{\hbar} g W_{i,f}^2 \sum_m w_m \sum_n |\langle \chi_{im} | Q - Q_0 | \chi_{fn} \rangle|^2 \times \delta(\Delta E + m\hbar\Omega_i - n\hbar\Omega_f), \quad (1)$$

where $f(T)$ is a scaling factor which depends on the charge state of the defect and temperature T [21], g is the degeneracy of the final state, $W_{i,f}$ are the electron-phonon coupling matrix elements, w_m is the thermal occupation of the vibrational state m , Q_0 is the shift between the adiabatic potentials, ΔE is the transition energy, and $\Omega_{i,f}$ are the vibrational frequencies of the initial (excited) and the final (ground) states, respectively. In the case of Be_{Ga} acceptor, we find the polaronic and ground state vibrational energies $\hbar\Omega_{i,f}$ to be very similar at ~ 36 meV (obtained from direct HSE calculations, filled circles in Fig. 2). The electron-phonon coupling matrix elements are calculated using HSE as

$$W_{i,f} = (\varepsilon_f - \varepsilon_i) \left\langle \psi_i \left| \frac{\partial \psi_f}{\partial Q} \right. \right\rangle, \quad (2)$$

where single-particle wave function ψ_i corresponds to the hole (electron) in the valence (conduction) band perturbed by the defect, ψ_f corresponds to the carrier localized on the defect, and $\varepsilon_{i,f}$ are the corresponding eigenvalues. This approach can be used to calculate both the nonradiative capture of the hole by the deep polaronic state C_p^d and the nonradiative capture of the electron by the ground state C_n^{NR} in Fig. 2.

The radiative transition rates (and corresponding capture coefficients) can be calculated from the Fermi's golden rule for the optical transition between the conduction band and the localized defect state [29]:

$$r = \frac{4}{3} \frac{\alpha n \Delta E}{\hbar m^2 c^2} |\langle \psi_c | \hat{p} | \psi_d \rangle|^2, \quad (3)$$

where α is the fine structure constant, n is the index of refraction, ΔE is the transition energy, m is the free electron mass, $\psi_{c,d}$ are the single-particle Kohn-Sham orbitals of the electron in the conduction band and the defect state, respectively, and \hat{p} is the momentum operator. The transition rates are calculated in the equilibrium geometries of the deep and shallow states of the neutral acceptor, for the transition energies corresponding to the computed PL maxima.

The results for the calculated capture coefficients are summarized in Table I. The radiative electron capture coefficient by the polaronic state C_n^d is calculated to be 10^{-13} cm³/s, which would determine the lifetime of PL from the polaronic state. The nonradiative capture of an electron by the polaronic state is hindered by the potential barrier, and for the HSE computed potentials (filled circles in Fig. 2) at low temperature C_n^{NR} is calculated to be 10^{-19} cm³/s. This low value stems from the significant width of the potential barrier for this transition (Fig. 2), suggesting that transitions via the polaronic state should be radiative, leading to a red PL band. This indeed would be the case, if only one state of neutral acceptor existed for

TABLE I. Carrier capture coefficients for Be_{Ga} acceptor in units of cm³/s.

	Shallow state	Deep (polaron) state
Nonradiative hole capture	$C_p^s \sim 10^{-6}-10^{-5}$	$C_p^d = 10^{-7}$
Nonradiative electron capture	Not applicable	$C_n^{\text{NR}} = 10^{-19}$
Radiative electron capture	$C_n^s \sim 5 \times 10^{-12}$	$C_n^d = 10^{-13}$

Be_{Ga}. However, the efficiency of the radiative transitions is also determined by the competition for a photogenerated hole between the shallow and deep states. Both states capture the hole without a barrier (Fig. 2). The hole capture coefficient by the deep state C_p^d , calculated using Eq. (1), is 10^{-7} cm³/s. Note that thus calculated C_p for a common acceptor in GaN, carbon acceptor C_N (assuming hole capture without a barrier, as observed in the experiment [30]), is also about 10^{-7} cm³/s, in agreement with the measured value of 3×10^{-7} cm³/s [30]. The capture of a hole by the shallow state (C_p^s) cannot be accurately calculated from first principles, because Eqs. (1) and (2) require evaluation of the single-particle wave functions, which are too extended to be reproduced in a supercell calculation of any reasonable size. For the same reason, in our HSE calculations the shallow state transition level is an overestimated 0.24 eV vs measured 0.11 eV. It is, however, known from the experiment that C_p^s for another shallow acceptor in GaN (magnesium acceptor Mg_{Ga}) is 10^{-6} cm³/s [28,30]. It should also be noted that the shallow state of Mg_{Ga} (0.2 eV above the VBM) is deeper than that of Be_{Ga} (0.11 eV), indicating that Be_{Ga} defect state wave function is significantly more extended. Roughly C_p^s can be estimated as $C_p^s = 4 \pi Z e \mu / \kappa$, based on the carrier capture by a shallow attractive center limited by diffusion [31]. Here, Z is the defect formal charge, e is the electron charge, μ is the hole mobility, and κ is the bulk GaN dielectric constant. Within this approximation, the hole capture coefficient for the shallow state is estimated between 10^{-6} and 10^{-5} cm³/s, for the hole mobilities of 3–30 cm²/(V s) [32,33]. In other words, the shallow state of Be_{Ga} acceptor is 1–2 orders of magnitude more efficient at capturing photogenerated holes as compared to the polaronic state. Thus, upon optical excitation, the holes are predominantly captured by the shallow state, with subsequent PL in the UV region (the computed radiative electron capture coefficient C_n^s is 5×10^{-12} cm³/s). The holes can also be captured by the polaronic state but at a significantly lower rate. This leads to the predicted PL intensity from the polaronic state lower, at least by 1–2 orders of magnitude, than that from the UVL_{Be} band. In the experiment, the ratio of the peak intensities would be even larger, because the PL band from the polaronic state is expected to be significantly broader than the UVL_{Be} band. Furthermore, the ratio of PL intensities related to the shallow and deep polaronic states must be the same in

semiconductors with arbitrary compositions of defects, including n -type and p -type samples. Indeed, in the Shockley-Read-Hall phenomenological approach [34–36], these intensities are $I_s^{\text{PL}} = C_p^s N_A^- p$ and $I_d^{\text{PL}} = C_p^d N_A^- p$, respectively, where N_A^- is the concentration of negatively charged Be_{Ga} acceptors and p is the concentration of free holes. Then $I_s^{\text{PL}}/I_d^{\text{PL}} = C_p^s/C_p^d$, independent of a specific sample. The same should be true for other defects with the dual nature, such as Mg and Zn acceptors in GaN or Li acceptor in ZnO [5].

In conclusion, PL measurements of optical transitions via the Be_{Ga} acceptor in GaN show that the Be_{Ga} has a shallow, effective-mass-like state with the 0/– transition level at 113 ± 5 meV, which is responsible for the UVL_{Be} band with the main peak at 3.38 eV. This means that the Be_{Ga} forms the shallowest acceptor level in GaN known to date. This result is encouraging, particularly for AlGaIn-based devices, where the concentration of free holes in p -type AlGaIn alloy remains frustratingly low because of the large ionization energy of the Mg_{Ga}. The HSE calculations predict the dual nature of the Be acceptor, with the shallow state responsible for the UVL_{Be} and a deep small polaronic state at 0.58 eV above the VBM, which is not observed in PL experiments. Calculated carrier capture coefficients suggest that the small polaron is significantly less efficient at capturing photogenerated holes than the shallow state. Therefore, the expected red PL band from the small polaron would be significantly lower in intensity than the UVL_{Be} band. In the experiment it would also likely be buried under the bright YL_{Be} band observed in the same region of the spectrum, making it especially challenging to resolve. Remarkably, the existence of the “bright” shallow state and the “dark” polaronic state of an acceptor appears to be a general phenomenon. The situation is similar for the Mg_{Ga}, Zn_{Ga}, Cd_{Ga}, and Ca_{Ga} acceptors in GaN, where the theory predicts deep polaronic states, while they are not observed in PL experiments.

This work was supported by the National Science Foundation (DMR-1904861). The calculations were performed at the VCU Center for High Performance Computing.

[1] H. Morkoç, *Handbook of Nitride Semiconductors and Devices: Electronic and Optical Processes in Nitrides* (John Wiley & Sons, New York, 2009).

- [2] M. A. Reshchikov and H. Morkoç, *J. Appl. Phys.* **97**, 061301 (2005).
- [3] J. L. Lyons, A. Janotti, and C. G. Van de Walle, *Jpn. J. Appl. Phys.* **52**, 08JJ04 (2013).
- [4] X. Cai, J. Yang, P. Zhang, and S.-H. Wei, *Phys. Rev. Applied* **11**, 034019 (2019).
- [5] S. Lany and A. Zunger, *Appl. Phys. Lett.* **96**, 142114 (2010).
- [6] S. Lany and A. Zunger, *Phys. Rev. B* **81**, 205209 (2010).
- [7] S. Lany, *Phys. Status Solidi (b)* **248**, 1052 (2011).
- [8] T. Gake, Y. Kumagai, and F. Oba, *Phys. Rev. Mater.* **3**, 044603 (2019).
- [9] A. Salvador, W. Kim, Ö. Aktas, A. Botchkarev, Z. Fan, and H. Morkoç, *Appl. Phys. Lett.* **69**, 2692 (1996).
- [10] D. J. Dewsnip, A. V. Andrianov, I. Harrison, J. W. Orton, D. E. Lacklison, G. B. Ren, S. E. Hooper, T. S. Cheng, and C. T. Foxon, *Semicond. Sci. Technol.* **13**, 500 (1998).
- [11] F. J. Sánchez, F. Calle, M. A. Sánchez-García, E. Calleja, E. Muñoz, C. H. Molloy, D. J. Somerford, J. J. Serrano, and J. M. Blanco, *Semicond. Sci. Technol.* **13**, 1130 (1998).
- [12] K. Lee, B. L. VanMil, M. Luo, L. Wang, N. C. Giles, and T. H. Myers, *Phys. Status Solidi (c)* **2**, 2204 (2005).
- [13] A. J. Ptak, T. H. Myers, L. Wang, N. C. Giles, M. Moldovan, C. R. D. Cunha, L. A. Hornak, C. Tian, R. A. Hockett, S. Mitha, and P. V. Lierde, *MRS Online Proc. Library Archive* **639**, G3.3 (2000).
- [14] H. Teisseyre, J. L. Lyons, A. Kaminska, D. Jankowski, D. Jarosz, M. Boćkowski, A. Suchocki, and C. G. Van de Walle, *J. Phys. D* **50**, 22LT03 (2017).
- [15] H. Teisseyre, M. Bockowski, I. Grzegory, A. Kozanecki, B. Damilano, Y. Zhydachevskii, M. Kunzer, K. Holc, and U. T. Schwarz, *Appl. Phys. Lett.* **103**, 011107 (2013).
- [16] W. R. Willoughby, M. E. Zvanut, J. Dashdorj, and M. Bockowski, *J. Appl. Phys.* **120**, 115701 (2016).
- [17] W. R. Willoughby, M. E. Zvanut, and M. Bockowski, *J. Appl. Phys.* **125**, 075701 (2019).
- [18] See Supplemental Material at <http://link.aps.org/supplemental/10.1103/PhysRevLett.126.027401> for details on the experimental and theoretical methods, which includes Refs. [19–26].
- [19] M. A. Reshchikov, M. Vorobiov, D. O. Demchenko, Ü. Özgür, H. Morkoç, A. Lesnik, M. P. Hoffmann, F. Hörich, A. Dadgar, and A. Strittmatter, *Phys. Rev. B* **98**, 125207 (2018).
- [20] J. Heyd, G. E. Scuseria, and M. Ernzerhof, *J. Chem. Phys.* **118**, 8207 (2003).
- [21] A. Alkauskas, Q. Yan, and C. G. Van de Walle, *Phys. Rev. B* **90**, 075202 (2014).
- [22] D. O. Demchenko, I. C. Diallo, and M. A. Reshchikov, *Phys. Rev. B* **97**, 205205 (2018).
- [23] F. Tuomisto, V. Prozheeva, I. Makkonen, T. H. Myers, M. Bockowski, and H. Teisseyre, *Phys. Rev. Lett.* **119**, 196404 (2017).
- [24] K. Lee, Issues for *p*-type doping of gallium nitride with beryllium and magnesium grown by rf-plasma assisted molecular beam epitaxy, Ph.D. thesis, West Virginia University, 2007.
- [25] C. G. Van de Walle and J. Neugebauer, *J. Appl. Phys.* **95**, 3851 (2004); C. Freysoldt, B. Grabowski, T. Hickel, J. Neugebauer, G. Kresse, A. Janotti, and C. G. Van de Walle, *Rev. Mod. Phys.* **86**, 253 (2014).
- [26] C. Freysoldt, J. Neugebauer, and C. G. Van de Walle, *Phys. Rev. Lett.* **102**, 016402 (2009); *Phys. Status Solidi (b)* **248**, 1067 (2011).
- [27] K. Kornitzer, T. Ebner, K. Thonke, R. Sauer, C. Kirchner, V. Schwegler, M. Kamp, M. Leszczynski, I. Grzegory, and S. Porowski, *Phys. Rev. B* **60**, 1471 (1999).
- [28] M. A. Reshchikov, P. Ghimire, and D. O. Demchenko, *Phys. Rev. B* **97**, 205204 (2018).
- [29] H.-S. Zhang, L. Shi, X.-B. Yang, Y.-J. Zhao, K. Xu, and L.-W. Wang, *Adv. Opt. Mater.* **5**, 1700404 (2017).
- [30] M. A. Reshchikov, A. Usikov, H. Helava, Yu. Makarov, V. Prozheeva, I. Makkonen, F. Tuomisto, J. H. Leach, and K. Udvary, *Sci. Rep.* **7**, 9297 (2017).
- [31] V. N. Abakumov, V. I. Perel', and I. N. Yassievich, *Non-radiative Recombination in Semiconductors* (North-Holland, Amsterdam, 1991).
- [32] P. Kozodoy, H. Xing, S. P. DenBaars, U. K. Mishra, A. Saxler, R. Perrin, S. Elhamri, and W. C. Mitchel, *J. Appl. Phys.* **87**, 1832 (2000).
- [33] Y. Arakawa, K. Ueno, A. Kobayashi, J. Ohta, and H. Fujioka, *APL Mater.* **4**, 086103 (2016).
- [34] W. Shockley and W. T. Read, Jr., *Phys. Rev.* **87**, 835 (1952).
- [35] R. N. Hall, *Phys. Rev.* **87**, 387 (1952).
- [36] M. A. Reshchikov, A. A. Kvasov, M. F. Bishop, T. McMullen, A. Usikov, V. Soukhoveev, and V. A. Dmitriev, *Phys. Rev. B* **84**, 075212 (2011).